**Alex Pokryvailo, Costel Carp, and Clifford Scapellati**

*Spellman High Voltage Electronics Corporation*
*475 Wireless Boulevard*
*Hauppauge, NY 11788*

# *Comparative Testing of Simple Terminations of High-Voltage Cables*

# Comparative Testing of Simple Terminations of High-Voltage Cables

**Key words:** high-voltage cable, direct current, polyethylene insulation, shrink tubes, stress grading tapes, corona, space charge

**Alex Pokryvailo, Costel Carp, and Clifford Scapellati**
*Spellman High Voltage Electronics Corporation*
*475 Wireless Boulevard*
*Hauppauge, NY 11788*

*In high-voltage cable terminations, leakage currents often originate from the ground shield. Design factors significantly influence their magnitude and temporal behavior.*

## Introduction

In HV systems, cable terminations are one of the weakest links. The majority of failures occur on the ground shield side. This side is especially stressed by the electric field in free space connections. Field control and rigorous technological processes are key to reliable functioning. The first was realized for a century by stress relief cones in conjunction with solid dielectric fillings. Later, stress-grading nonlinear materials in the form of paint, tapes, and tubes were used with much success (see, e.g., [1]–[3] and their bibliography). In dc applications, which are the main interest of this paper, the falling resistivity-field characteristic effectively pushes the electric field off the shield terminus, where it is strongest.

Many field calculations for cable terminations have been published, analytical and numerical, using both linear and nonlinear approaches [1]–[6]. Understandably, they did not address the space charge formation arising from ionization around sharp edges. In fact, most designs avoid fields strong enough to cause ionization. It also seems that little or no work has been done on leakage current (LC) flowing along the cable termination. In low-current, precision HV applications, these currents may be comparable with the load current, and being inherently unstable, can compromise stability. At the same time, low-cost design limits the use of high-quality materials and/or elaborate field control techniques. These limitations are especially important in open-space connections characterized by very unfavorable stress concentration at the shield terminus.

In this light, several termination types for polyethylene HV cables were tested for dielectric strength and LC, down to the picoampere level. It was not the goal of this work to investigate partial discharge (PD) phenomena, in the cable body or in its terminations, although we are fully aware of possible correlation between PD and LC.

## Experimental Setup

This section describes the layout of the test setup, the design of the tested cables, and the experimental routines.

### *Test Rig*

The test bench (Figure 1) comprises a test power supply unit (PSU) V1 with its HV cable T1, cable under test (CUT) T2, and measurement and data-acquisition equipment. Two PSUs (Spellman SL130kV and XRF180kV series) provide smooth voltage regulation and high stability in the range 0–130 kV and 0–180 kV for positive and negative polarities, respectively. The HV leads of the CUT and the PSU cable are connected together, whereas the CUT shield is grounded through a current-measuring device (Keithley picoammeter 6487). A typical physical implementation is shown in Figure 2.

High-voltage leads of all cables were connected physically to the HV electrode of a voltage divider (Spellman model HVD-100) [7] capable of corona suppression up to 130 kV, as suggested by electric field analysis. In this way, the LCs generated by the ionization (corona) mechanism at the CUT *shield side only* are collected and directed through the picoammeter. To exclude the current originating at the lead end of the CUT, we screened its shield by a grounded copper electrode.

 *0883-7554/07/$25/©2010IEEE* 

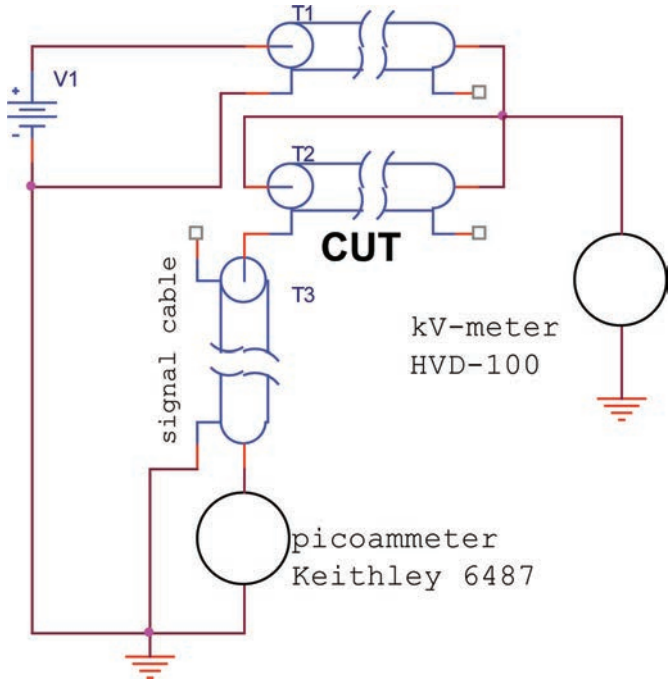


*Figure 1. Schematic layout of test rig.*

**Table 1. CUTs Description.**

| CUT designation | Termination method | Termination length l (Figure 3d, f), cm |
|---|---|---|
| (CUT#1) | FC, no SHT | 20 |
| (CUT#2) | FC, SHT | 20 |
| (CUT#3) | FC, SHT | 14.7 |
| (CUT#4) | O-ring cross-section diameter 2 mm, SHT | 14.7 |
| CUT#5 | Shield flapped over protective jacket, tape 217.21 | 14.7 cm, 3 cm from shield covered by 217.21 |
| CUT#6 | Shield flapped over, HiK 6501 | 14.7 cm, 3 cm from shield covered by tape HiK 6501 |

## *CUTs*

Several CUTs were manufactured from a 2124 Dielectric Sciences Polyethylene (PE) cable. All of them were approximately 2.5 m long. Their main parameters are summarized in Table 1, and photos of several of them are shown in Figure 3. The acronyms FC and SHT stand for flush cut and shrink tube, respectively (Alpha Wire Company irradiated polyolefin SHTs were used). Semiconductive stress-grading tape VonRoll 217.21 is SiC based and exhibits nonlinear behavior. Its conductivity increases at higher fields, effectively suppressing corona. HiK 6501 tape from Dielectric Sciences is defined as conductive. However, its resistivity was too large to be measured at low voltage using digital voltmeters. Its datasheet is unavailable.

## *Test Procedure*

For LC, every cable was tested in steps of, typically, 10 kV up to 90 kV and steps of 5 kV above 90 kV. CUT#6 was not tested

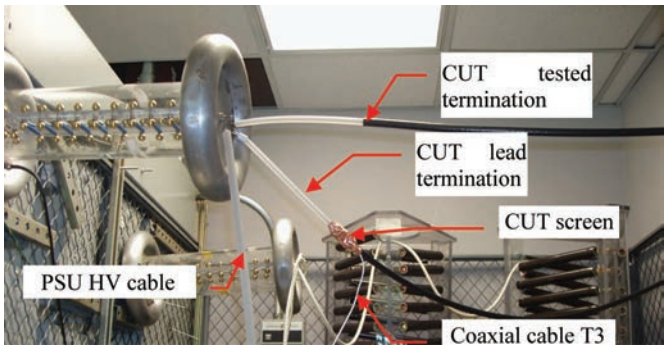


*Figure 2. Experimental setup.*

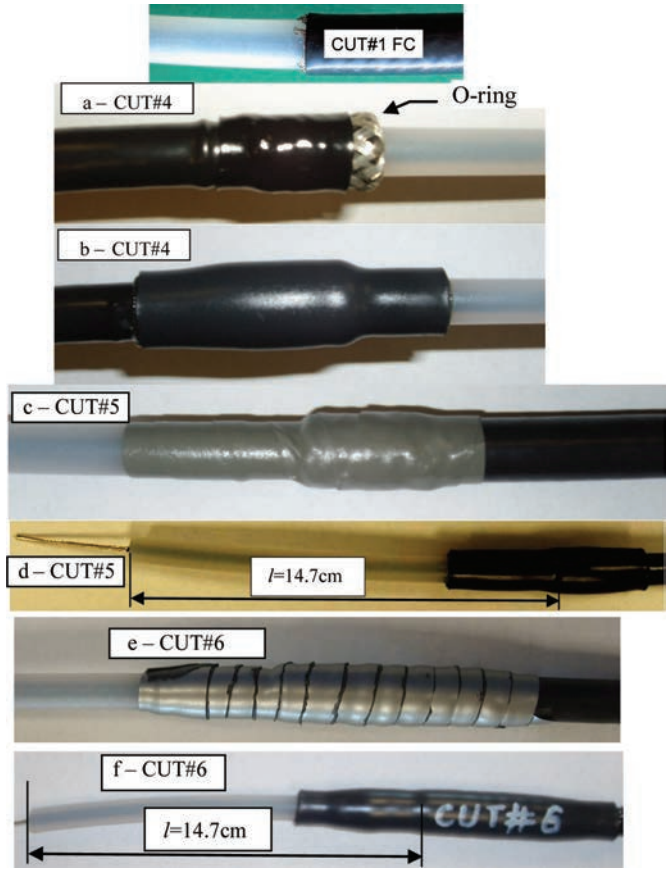


*Figure 3. CUT#1 showing loose strands. a) CUT#4, shield flapped over protective jacket and held by shrink tube (SHT); b) CUT#4, additional SHT cover; c) CUT#5, shield flapped over jacket and held by semiconductive tape Von Roll 217.21 protruding ~3 cm onto bare polyethylene (PE); d) CUT#5 ready for test, SHT cover on top of semiconductive tape; e) CUT#6, shield flapped over and held by HiK 6501 protruding ~3 cm onto bare PE; f) CUT#6 ready for test, SHT cover on top of HiK tape.*

at negative polarity. It is important to note that the voltage was changed monotonously, always increasing. Every test voltage was applied a minute before collecting the LC data transferred from the Keithley picoammeter to a PC using Keithley ExceLINX software. Thirty-five values were collected and stored at each measurement, which lasted 46 s, and averaged. Volt-ampere characteristics were constructed from the averages.

Ambient temperature and humidity were typically 25°C and 60 %, respectively. They were not monitored, but it is unlikely that they varied significantly during data collection.

CUTs#3, 4, 5, and 6 were subjected to breakdown voltage tests. The voltage was raised at a rate of approximately 2 kV/s to breakdown and then reduced to a level at least 20 kV lower than the registered breakdown voltage. The test was repeated 2 to 4 times. In view of the damage sustained by the shrink insulation and semiconductive tape, these were replaced before testing with the opposite polarity. Given the small number of samples, no averaging or other statistical processing was applied to the disruptive test data. The flashover was videotaped to document the flashover pattern.

## Experimental Results

### *Leakage Current Measurement*

To establish a baseline, the first measurements were conducted on the FC bare cable CUT#1. The LC was stable in time, especially at positive polarity voltages (grounded shield negative) higher than 20 kV, as shown in Figure 4a. The LC reached 40 μA at +90 kV and 98 μA at –90 kV (Figure 4b). To ensure that the current did indeed originate at the *cable shield*, an additional experiment was conducted in which the FC was protected by a relatively low-curvature electrode. This reduced the current to less than 3 μA at +90 kV. Obviously, the current was generated by a corona discharge.

Covering the shield termination by SHT suppressed the leakage by orders of magnitude (Figure 5), especially at positive polarity, which also confirms the origin of the leakage current as the shield cut of the *tested termination* end. Reducing the length of the bare PE to $l$ = 14.7 cm in CUT#3 resulted in somewhat higher leakage. The height of the error bars in these and similar plots is the standard deviation calculated over all 35 measurements. Using an O-ring termination (CUT#4) with SHT, of the same length as the bared PE, caused the LC to drop by an order of magnitude, compared with the FC of CUT#3 (Figure 6), at both polarities (compare with Figure 5).

CUT#5 with semiconductive tape and CUT#6 with HiK tape (Figure 7) had the lowest LCs, of order 1 nA at 100 kV at *positive* polarity. Also, the currents increased fairly smoothly with increasing voltages, i.e., there were very few picoammeter overflows on the 200-nA range, whereas other cables could be tested only on the 20-μA range at 100 kV. CUT#5 was also tested at negative polarity. The LC was large (Figure 8), even higher than that of CUT#4 (Figure 6).

The negative-polarity LCs were always higher than those at positive polarity. The reasons for this are discussed in the Analysis and Discussion section.

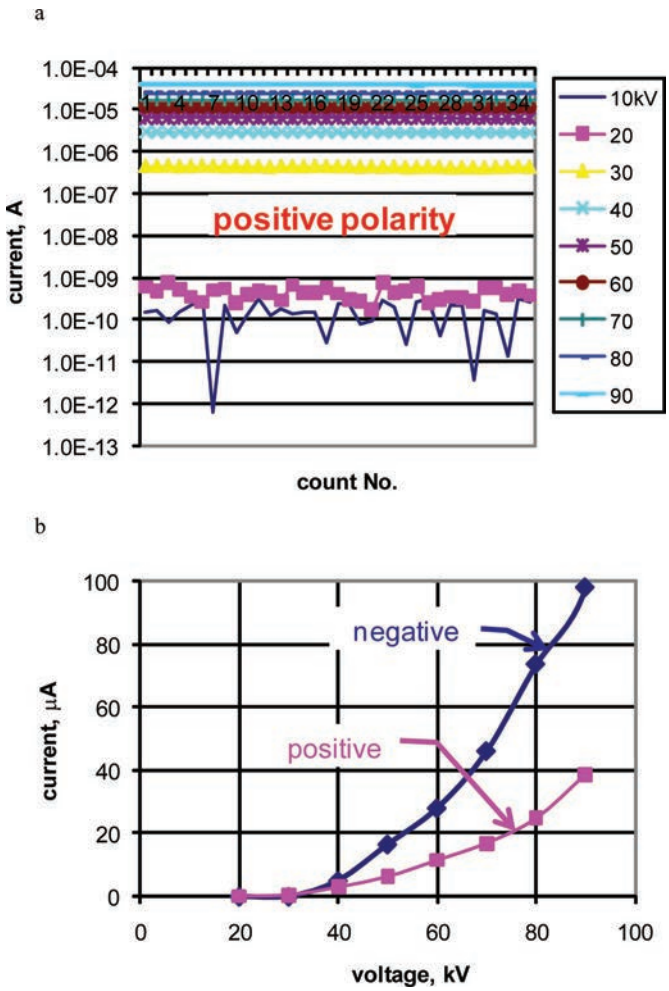


*Figure 4. Leakage current (LC) for CUT#1 (flush cut, no shrink tube). a) LC dependence on time (count number) at positive polarity; b) LC as a function of applied voltage at positive and negative polarity.*

### *Breakdown Voltage Tests*

The tests were conducted as indicated in the Test Procedure section.

At *positive polarity*, for CUT#3, the first flashover occurred at 104 kV along the surface of the test termination. The subsequent breakdowns (at 124 kV) occurred along the surface of the much longer *lead* termination. The path change may be attributed to conditioning of the shield, i.e., removal of loose strands by the arc.

CUT#4 had a different flashover pattern, with the spark bridging the shield and the HV electrode of the HVD-100 voltage divider through the air (Figure 9). First breakdown was at 124.5 kV, and subsequent ones were at 112, 113, and 117 kV. CUT#5 and CUT#6 behaved very similarly to each other but very differently from the other specimens. They broke down at 130 kV after ~10 s exposure. The first flashover reached the folded end of the shield, as indicated by the arrow in Figure 10. Consecutive breakdowns occurred at the same voltage, but the luminous channel ended at the shrink sleeve end.

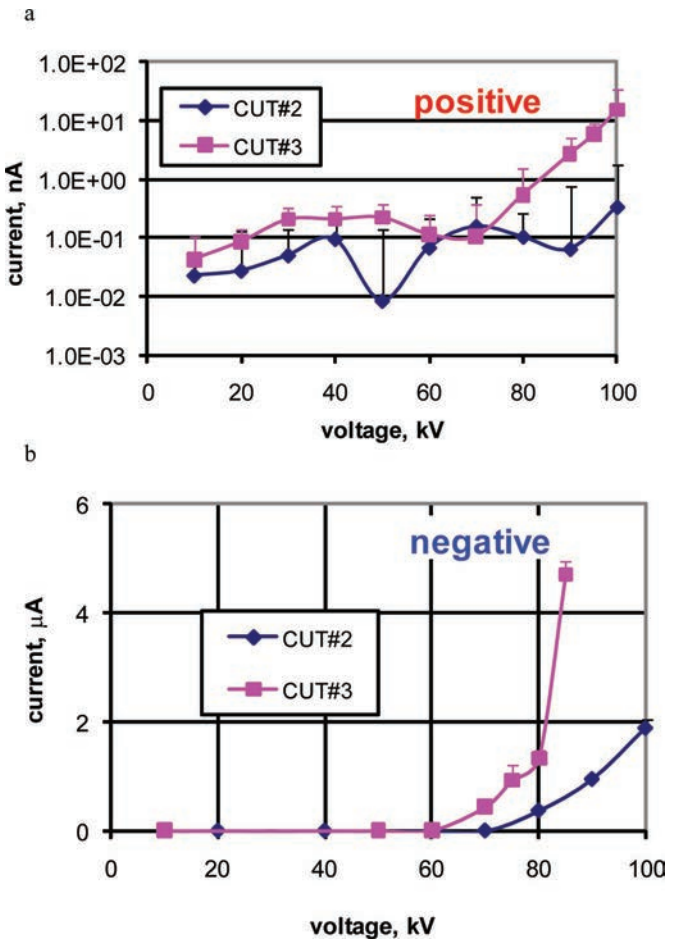


*Figure 5. Leakage current as a function of applied voltage for CUT#2 [flush cut (FC), shrink tube (SHT), l = 20 cm polyethylene bared length] and CUT#3 (FC, SHT, l = 14.7 cm) at (a) positive and (b) negative polarity.*

At *negative polarity*, CUT#4 flashed over the PE surface, with the spark anchored at the O-ring. The first breakdown was at 126 kV, and subsequently at 109 and 104 kV, almost identical to the positive-polarity case. CUT#5 broke down at 136 kV after ~5 s exposure. The first flashover reached the folded end of the shield, as indicated by the arrow in Figure 11. The second breakdown occurred at the same voltage, but intense corona started forming at 80 kV. The other cables were not tested at negative polarity.

## Analysis and Discussion

The cable-insulating system comprising PE, SHT, and air is difficult to analyze because of its ill-defined geometry and the nonlinear electrical characteristics of some of the materials. Thus, accurate electric field calculations are difficult, if not impossible. However, several general features can be observed.

In dc systems, conduction currents govern the field distribution, but displacement currents are more important during fast transient processes and under ac conditions (50 Hz and higher). In other words, the material *conductivity* is dominant at dc, but the material *permittivity* is dominant at ac. This is now well recognized [8]-[11].

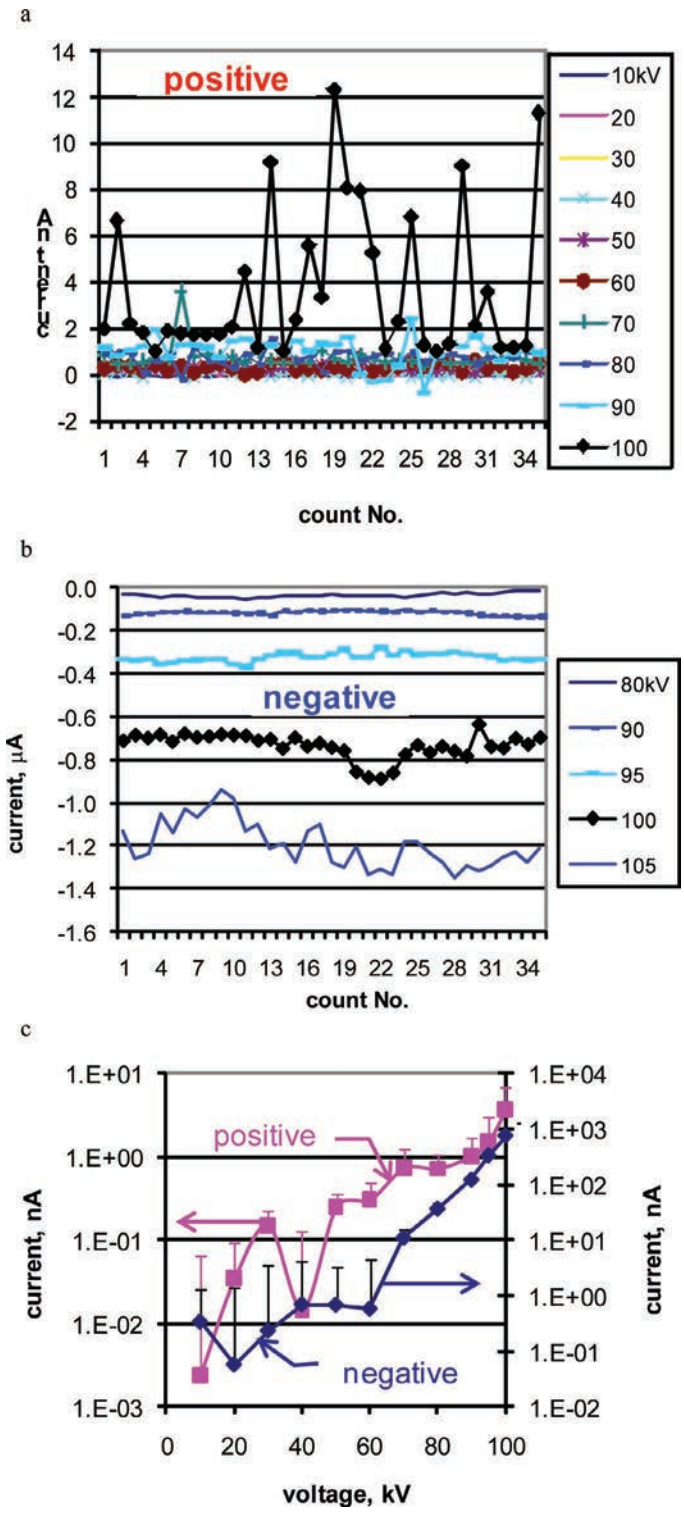


*Figure 6. Leakage current (LC) of CUT#4 (O-ring, shrink tube). a) LC dependence on time (count number) at positive polarity; b) same at negative polarity; c) LC as a function of applied voltage at positive and negative polarity.*

The differences in the field distribution can be seen in Figures 12, 13, and 14, which were generated using Ansoft Maxwell 2D Student Version [12]. The assumed geometry approximates that

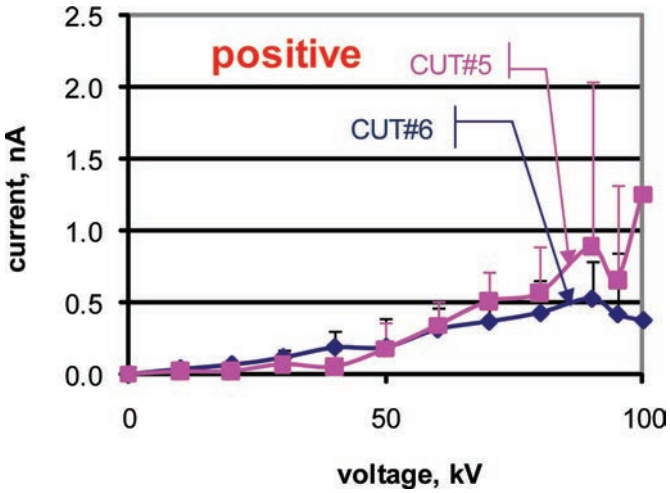


*Figure 7. CUT#5, CUT#6. Leakage current at positive polarity.*

of the test arrangement (see Figure 2). In all calculations, the potential difference between the HV electrodes and ground was 1 V. Because we are dealing with a linear problem, the results can be scaled with the applied voltage. Plots a and b correspond to the dc and ac cases, respectively. In the former, the ratio of PE resistivity to that of air was taken as 100, and in the latter, the relative permittivity of PE was set at 2.25. The field under ac is much less uniform. The dc distribution is greatly influenced by the temperature dependence of the component conductivities. Irrespective of the applied voltage waveform, the field may be further modified by ionization processes and reduced or enhanced by space and surface charges. At negative polarity on the sharp electrode, space charge tends to reduce the maximum field. Semiconductive tapes have the same effect under *both* polarities, suppressing ionization and improving LC stability.

Obviously, the high fields predicted by the field analysis for FC without SHT (E >100 kV/cm for both cases at a voltage greater than 60 kV) would lead to air ionization. This is manifested by CUT#1 with exposed shield and short (~1 mm) loose strands protruding outward from it randomly, which lead to further field enhancement. Clearly, large currents drawn from the shield (Figure 4) are generated by a mechanism similar to corona, which may also be described as creeping discharge. Currents became measurable at voltages above 30 kV for both polarities. Scaling Figure 13a up to 30 kV suggests a field of 50 kV/cm at this voltage, which surprisingly agrees with the values for the corona onset fields, in similar air gaps, given on page 153 of [13]. In agreement with published data [13], [14], *at the same applied voltage*, the corona current is greater for positive polarity of the sharp electrode (shield) or, in the terminology of this article, at negative polarity. It should be further emphasized that although positive corona draws larger current than its negative counterpart, the difference in a unipolar corona mode is small, in the range of 20–30%. The reason is that the mobilities of positive and negative ions are very similar in electronegative gases. Positive streamer corona developing at higher voltages in large gaps tends to draw much larger current but transits to spark at lower voltage than negative corona [15]. This effect is related to the streamer mechanism of discharge described in [14] and [16].

If the SHT resistivity is lower than that of PE, the field at the shield edge is weakened considerably (Figure 14), below the corona onset level. This might partially explain the dramatic improvement brought about by the SHT covering. Here we adopted the figures of $10^{14}\,\Omega\cdot$m [17], $10^{12}\,\Omega\cdot$m [18], and $10^{13}\,\Omega\cdot$m for the resistivities of PE, SHT, and air, respectively. Beyer *et al.* [19] cited a resistivity of $4\cdot10^{14}\,\Omega\cdot$m for air at STP, but we have used $10^{13}\,\Omega\cdot$m in view of the fact that the gas resistivity is higher in the absence of ionization. Note that the term *resistivity* must be applied cautiously because the current conduction is limited by saturation in a wide field strength range below the onset of impact ionization [14], [20], [21]. Shrink tube weakens the field because of its permittivity and conductivity values but generates only minor ionization in residual air pockets. The charges generated in this way are trapped and neutralize the external field, thus suppressing the ionization and greatly reducing the LC (Figure 5 and Figure 6). The sometimes erratic behavior of the LC curves is probably due to accumulation and decay of these charges, these processes frequently having large time constants because of the high resistivity of the dielectrics.

The O-ring termination reduces the external field and is superior to FC in that it is free of loose copper strands. The O-ring termination was effective at both polarities.

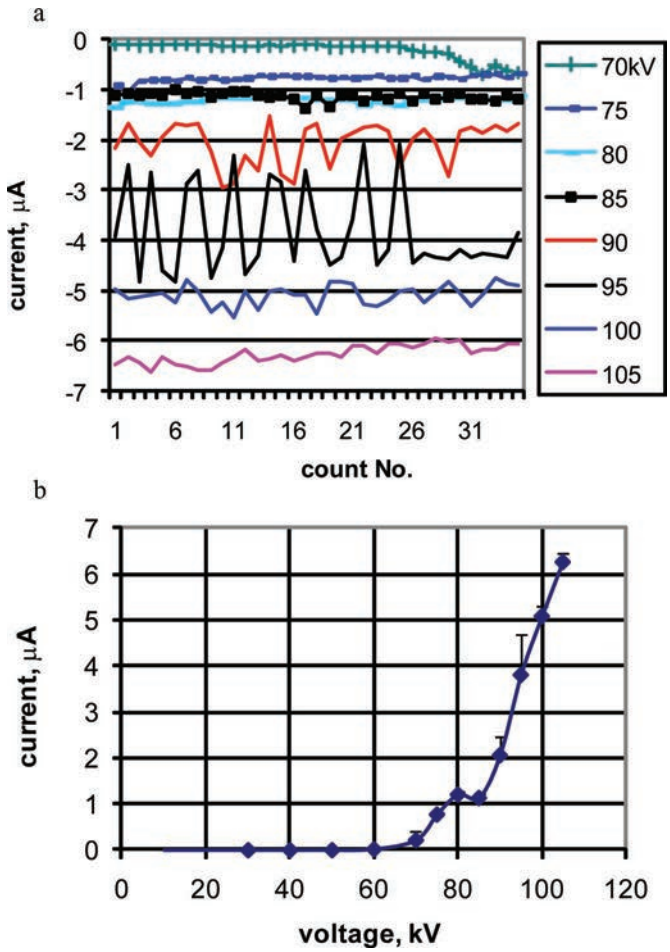


*Figure 8. CUT#5. Leakage current (LC) at negative polarity. a) LC dependence on time (count number); b) LC as a function of applied voltage.*

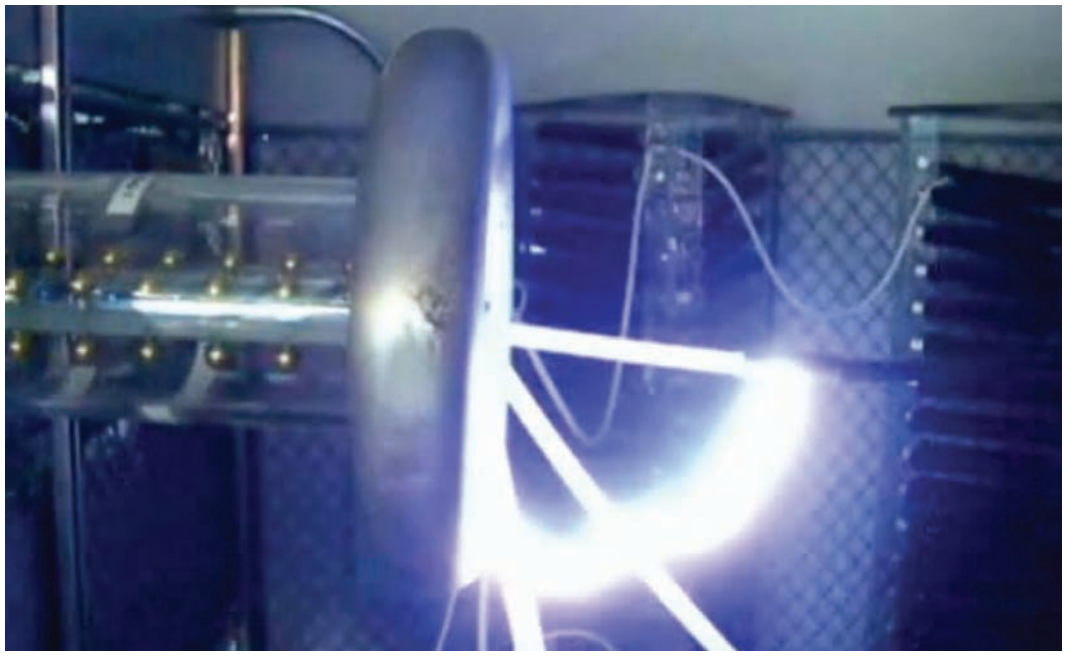

*Figure 9. CUT#4. Photo of flashover. Positive polarity.*

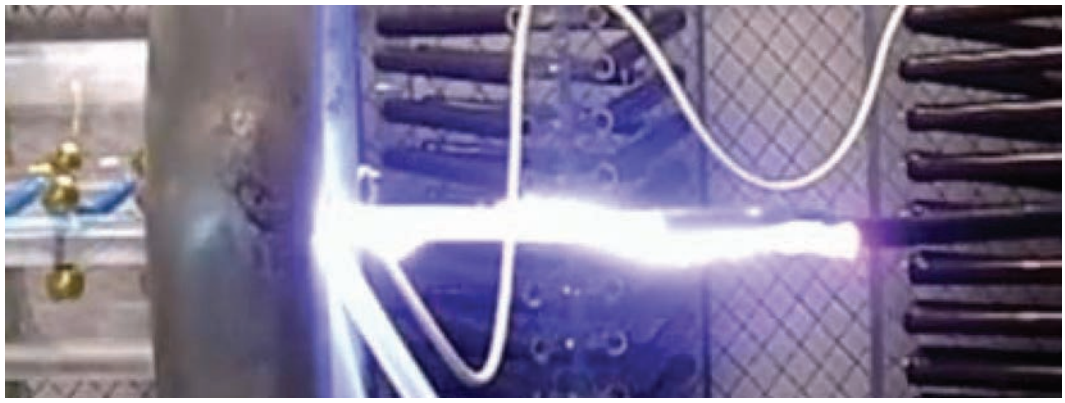

*Figure 10. CUT#5. Photo of flashover. Positive polarity.*

At negative polarity, the O-ring termination had lower LCs than the other CUTs. However, the breakdown voltage of CUT#5 was slightly higher than that of the O-ring termination. Because only 2 samples were tested, quantitative comparison is not useful. However, the flashover patterns for these designs are informative. For both polarities, the flashover followed the short path to the shield with FC and O-ring terminations but chose the long path in the case of the semiconductive and HiK tapes. Thus, the field at the shield termination is weakened by the tape, and so the breakdown voltage is higher.

Stress-grading tapes have the effect of pushing the field away from the shield. At positive polarity, CUT#5 and CUT#6 had very stable and low LCs. Their breakdown voltages were considerably higher than those of the other designs.

In our opinion, stress-grading tapes are not necessary for most dc applications but offer a major advantage for ac and pulsed applications.

For the cables equipped with SHTs, the LC at positive polarity was 3 orders of magnitude lower than that at negative polarity. We do not have a convincing explanation for this effect. Nu-

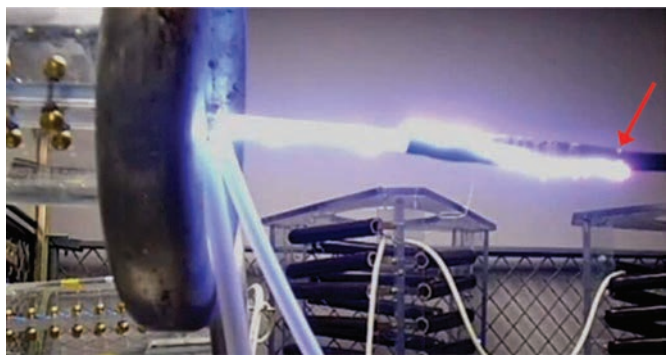

*Figure 11. CUT#6. Photo of flashover. Positive polarity.*

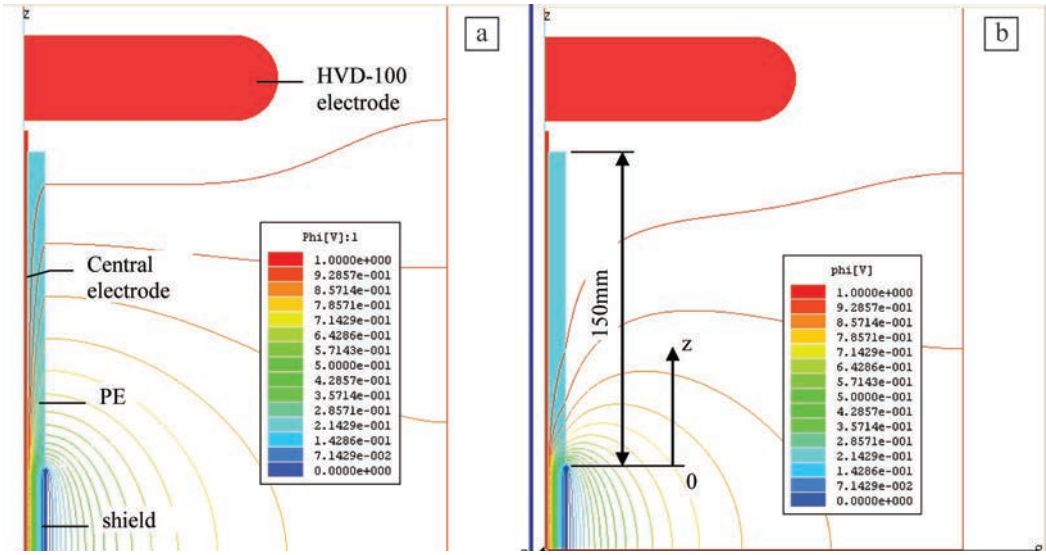


*Figure 12. Field plots (equipotential lines). a) dc field; b) ac field. Potential difference is 1 V.*

merous publications deal with the influence of dielectric barriers on the breakdown voltage of gas gaps, particularly in relation to polarity, barrier placement, identity of the gas, and its temperature and pressure [13], [14], [16], [19]-[23]. However, they do not discuss LCs.

Consider the influence of space charge on the discharge mechanism in gas gaps with strongly nonuniform electric fields. At negative polarity (positive shield), negative space charge attracted to the shield enhances the field, thus promoting the LC flow. On the other hand, at positive polarity, the same space charge is repelled and diffuses around the shield, effectively weakening the field and suppressing the LC.

As a rule, air gaps break down at nearly the same voltage in repetitive tests, provided the electrodes are not reconditioned, space charge, surface charge or metastables do not accumulate, and the ambient temperature is constant. Such effects were observed in high-repetition-rate pulsed discharges [24], [25]; the gap impedance increased and the breakdown voltage decreased at higher repetition rates. In our measurements, the breakdown voltages decreased markedly in consecutive tests, suggesting a different breakdown mechanism. The SHTs were punctured after several flashovers and, therefore, did not suppress LCs. It may be that at negative polarity and voltages at which the LCs reach several microamperes, the SHTs are damaged thermally following several flashovers as a result of localized power losses estimated at the subwatt level.

In the context of HV cable terminations, reducing and stabilizing LCs is essential for achieving higher breakdown voltages and greater reliability. There are other important considerations. The current drawn from the PSU is usually stable and is the sum of the load current and various LCs, including that of the cable. The data on the temporal behavior of the LCs presented in this work allow us to assess the level of the *load* current stability achievable under the cited ambient conditions. Thus, if the LC is of order 1 μA and the load current is 100 μA, one cannot expect stability better than 1%, even if the PSU stability is specified as 0.01%. Similar effects can be caused by dark currents in vacuum gaps [26].

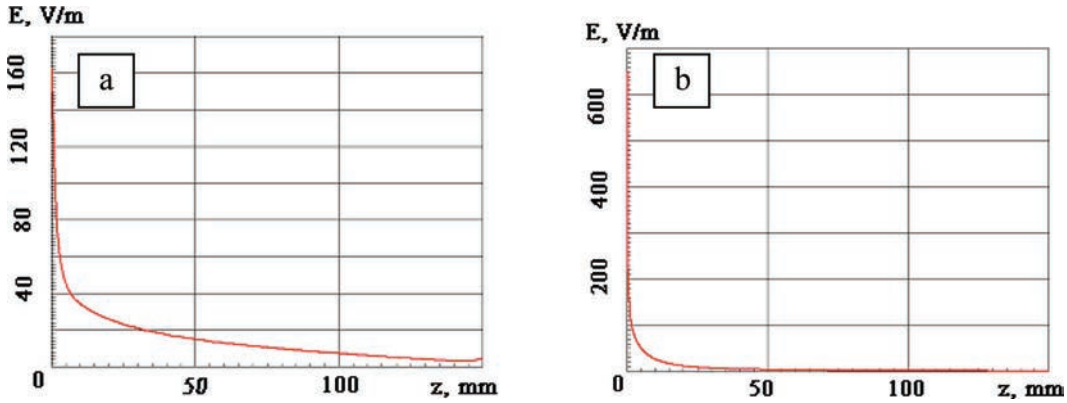


*Figure 13. E-field distribution along bare polyethylene starting from cable shield. Plots a and b correspond respectively to the dc and ac cases of Figure 12.*

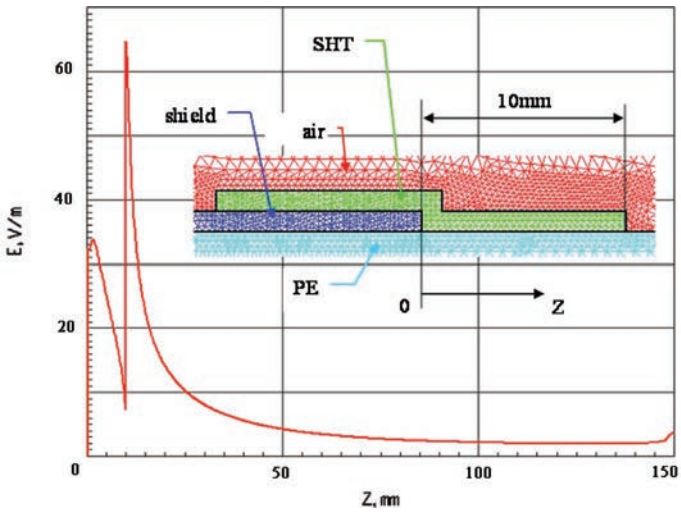


*Figure 14. E-field distribution along polyethylene (PE) starting from cable shield, dc case. Polyethylene covered by shrink tube (SHT) 1-mm thick. Inset shows part of meshed geometry. Resistivities of PE, SHT, and air are in the ratio of 100:1:10.*

## Conclusion

Six different types of 2124 cable shield termination were tested for leakage current and dielectric strength. The main results can be summarized as follows:

(1) Shrink sleeve strongly affects ionization phenomena, effectively suppressing corona discharge.

(2) Flush cutting a shield leaves loose short strands, which increase the probability of main insulation damage.

(3) Folding the shield back over an O-ring decreases the electric field strength, leaves no loose strands, and decreases the probability of main insulation damage. This is recommended for dc applications.

(4) Stress-grading tapes reduce (and greatly stabilize) leakage currents, at a level around 1 nA at 100 kV and room temperature. They also increase the breakdown voltage to approximately 130 kV for a 15-cm length of insulation. They are recommended for pulsed operation and critical dc applications.

## References


[1] P. N. Nelson and H. C. Hervig, "High dielectric constant materials for primary voltage cable terminations," *IEEE Trans. Power App. Syst.*, vol. PAS-103, no. 11, pp. 3211–321, Nov. 1984.

[2] J. C. G. Wheeler, A. M. Gully, A. E. Baker, and F. A. Perrot, "Thermal performance of stress grading systems for converter-fed motors," *IEEE Electr. Insul. Mag.*, vol. 23, no. 2, pp. 5–11, 2007.

[3] G. C. Stone, E. A. Boulter, I. Culbert, and H. Dhirani, *Electrical Insulation for Rotating Machines*. IEEE Press, Wiley, 2004.

[4] S. V. Nikolajevic, N. M. Pekaric-Nad, and R. M. Dimitrijevic, "Optimization of cable terminations," *IEEE Trans. Power Del.*, vol. 12, no. 2, pp. 527–532, April 1997.

[5] G. Lupb, K. Tucci, N. Femia, and M. Viielli, "Electric field calculation in HV cable terminations employing heat-shrinkable composites with non linear characteristics," in *Proceedings of the 4th International Conference on Properties and Applications of Dielectric Materials*, Brisbane, Australia, pp. 278–281, 1994.

[6] J. Mackevich and J. Hoffman, "Insulation enhancement with heat- shrinkable components. Part 111: Shielded power cable," *IEEE Electr. Insul. Mag.*, vo1. 7, no. 4, pp. 31–40, 1991.

[7] http://www.spellmanhv.com/~/media/Files/Products/HVD.ashx.

[8] P. Gallagher, *High Voltage: Measurement, Testing and Design*. Chichester, UK: Wiley, 1983, p. 197.

[9] A. I. Dolginov, *High Voltage Engineering*. Moscow: Energia, 1968.

[10] M. S. Khalil, "International research and development trends and problems of HVDC cables with polymeric insulation," *IEEE Electr. Insul. Mag.*, vol. 13, no. 6, pp. 35–47, 1997.

[11] A. Pokryvailo, "Analyzing electric field distribution in non-ideal insulation at direct current," in *Proc. Electrimacs 2008*, on CD-ROM, Quebec, Canada, June 2008.

[12] Maxwell 2D Student Version, Ansoft Corp., Pittsburgh, PA, 2002.

[13] J. M. Meek and J. D. Craggs, *Electrical Breakdown of Gases*. Oxford: Clarendon Press, 1953.

[14] L. B. Loeb, *Electrical Coronas: Their Basic Physical Mechanisms.* Berkeley: University of California Press, 1965.

[15] K. Parker, *Electrical Operation of Electrostatic Precipitators.* London: IEE, 2003.

[16] Y. P. Raizer, *Gas Discharge Physics.* Berlin: Springer, 1991.

[17] G. G. Raju, *Dielectrics in Electric Fields.* New York: Marcel Dekker Inc., 2003.

[18] Shrink Tubing. Available: http://www.alphawire.com/pages/114.cfm.

[19] M. Beuer, W. Boeck, K. Möller, and W. Zaengl, *Hochspannungstechnik.* Springer-Verlag, 1986, 1992. Translation to Russian 1989 (Moscow: Energoatomizdat).

[20] E. Kuffel and W. S. Zaengl, *High Voltage Engineering*, 2nd ed., Butterworth-Heinemann, 2000.

[21] G. I. Skanavi, *Physics of Dielectrics: Weak-Field Region.* Moscow: Gostekhizdat, 1949, pp. 218–219.

[22] G. I. Skanavi, *Physics of Dielectrics: Strong-Field Region.* Moscow: Fizmatlit, 1958.

[23] V. Y. Ushakov, *Insulation of High-Voltage Equipment* (*Power Systems*). Springer, 2004 (Translation from 1994 Russian ed.).

[24] Y. Yankelevich, R. Baksht, M. Wolf, A. Pokryvailo, J. Vinogradov, B. Rivin, and E. Sher, "NOx diesel exhaust treatment using pulsed corona discharge: The pulse repetition rate effect," *Plasma Sources Sci. Tech.*, vol. 16, pp. 386–391, 2007.

[25] A. Pokryvailo, M. Wolf, and Y. Yankelevich, "Investigation of operational regimes of a high-power pulsed corona source with an all-solid state pulser," *IEEE Trans. Dielectr. Electr. Insul.*, vol. 14, no. 4, pp. 846–857, Aug. 2007.

[26] A. Pokryvailo and V. Okun, "An investigation of stray currents of x-ray tubes having tubular hollow anodes," *Instrum. Methods X-Ray Anal.*, vol. 32, pp. 120–126, 1984 (in Russian).


**Alex Pokryvailo** was born in Vyborg, Russia. He received his MSc and PhD degrees in electrical engineering from the Leningrad Polytechnic Institute in 1975 and 1987, respectively. Formerly with Soreq NRC, Israel, he is now working with Spellman High Voltage Electronics Corp. His current and recent experience relates to pulsed power, with emphasis on high-current opening and closing switches and magnetic design, fast diagnostics, design of HV high-power switch-mode power supplies, and corona discharges. Previously he studied switching arcs, designed $SF_6$ insulated switchgear, and carried out research in the area of interaction of flames with electromagnetic fields. He has published over 100 papers and 2 textbooks (in Hebrew) and holds more than 20 patents pertaining to HV technology.